# Waste-free Soft Reactive Grinding Synthesis of High-Surface-Area Copper–Manganese Spinel Oxide Catalysts Highly Effective for Methanol Steam Reforming

Qian Liu · Lu-Cun Wang · Miao Chen ·
Yong-Meo Liu · Yong Cao · He-Yong He ·
Kang-Nian Fan

**Abstract** Cu–Mn spinel oxides with a high specific surface area were prepared by a simple and waste-free soft reactive grinding (SRG) technique involving the use of clean precursor salts as the starting materials. The samples were characterized by means of $N_2$ adsorption, X-ray diffraction (XRD), diffuse reflectance infrared Fourier transform spectroscopy (DRIFTS) and temperature-programmed reduction ($H_2$-TPR). The results show that the catalysts obtained from the SRG route exhibited much higher catalytic activity in methanol steam reforming as compared to their wet-chemically synthesized counterparts prepared by conventional coprecipitation. The superior performance of the SRG-derived Cu–Mn materials was attributed to the favorable formation of $Cu_{1.5}Mn_{1.5}O_4$ spinel phase leading to the creation of much smaller copper nanoparticles with enhanced stability in the working catalyst.

**Keywords** Waste-free · Soft reactive grinding (SRG) · Cu–Mn spinel oxides · Steam reforming of methanol · Hydrogen production

## 1 Introduction

Catalysts based on copper manganese mixed oxides are of great importance for catalytic processes like oxidation of carbon monoxide [1, 2], water–gas shift reaction [3], VOC removal [4], low-temperature NO reduction [5], and other
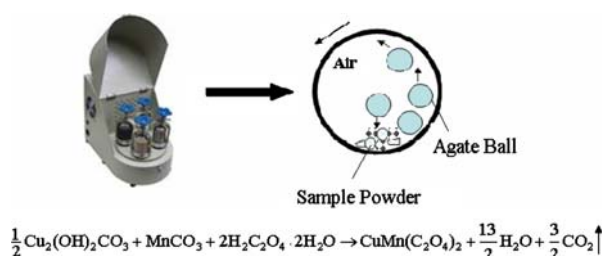
Q. Liu · L.-C. Wang · M. Chen · Y.-M. Liu · Y. Cao (✉) ·
H.-Y. He · K.-N. Fan
Department of Chemistry & Shanghai Key Laboratory
of Molecular Catalysis and Innovative Materials,
Fudan University, Shanghai 200433, P.R. China
e-mail: yongcao@fudan.edu.cn

industrially important hydrogenation and oxidation reactions [6–10]. It is also established that such materials are effective catalysts for steam reforming, particularly methanol steam reforming for clean fuel hydrogen production [11, 12]. As a result, Cu–Mn mixed oxides and their preparation have been extensively studied. The high activity of the Cu–Mn mixed oxide system is believed to result from a strong interaction of the CuO and $MnO_x$ phases leading to the formation of catalytically active copper–manganese spinel-phase in the Cu–Mn mixed oxide material [13]. Moreover, the enhanced activity associated with the nonstoichiometric Cu–Mn spinel oxides revealed the importance of textural or structural disorder of the copper–manganese mixed oxide materials [3, 4, 12–14].

Currently, several methods are available for the synthesis of copper–manganese mixed oxide catalysts [2–7, 11, 12]. Among them, coprecipitation routes via the hydroxycarbonate precursors are quite popular [4, 15, 16]. The most unsatisfactory aspect of the coprecipitation routes is the need of subsequent calcination at temperatures higher than 500 °C to induce the crystallization of Cu–Mn spinel phases, which however leads to undesirable sintering, grain growth, and dramatic loss of specific surface area in many cases [3, 4, 11, 12]. Moreover, the use of vast amounts of water as well as formation of large amounts of gaseous or liquid wastes presents additional environmental problems [17, 18]. In view of these circumstances, the development of new practical and environmental friendly synthetic methods for preparation of a high surface area copper–manganese spinel catalyst system is highly desirable.

Over the past decades, grinding-assisted catalyst synthesis has attracted tremendous attention by providing a much simpler, waste-free, easily scalable and energy-efficient technique for fabrication of new catalytic materials with improved and/or novel physical and chemical

properties as compared to conventional methods [19–25]. Very recently, we have shown that highly effective Cu/ZnO materials with favorable surface and structural properties for methanol steam reforming can be prepared via a simple yet versatile technique based on soft reactive grinding (SRG), removing the need of vast amount of water and the formation of large amount of wastes [26]. In the present study, we extend the scope of the SRG method to the synthesis of copper–manganese spinel oxide materials. We show that the SRG technique based on dry oxalate-precursors synthesis can allow a facile and waste-free preparation of Cu–Mn spinel materials with extremely high surface area, exhibiting much higher catalytic activity in methanol steam reforming than its conventional analogue prepared via coprecipitation route.

## 2 Experimental

### 2.1 Preparation of Catalyst

A typical SRG procedure to prepare the well-mixed Cu–Mn oxalate precursors is as follows: an 1:2 molar ratio amount of $Cu_2CO_3(OH)_2$ and $MnCO_3$ premixed with 20% stoichiometric excess of solid oxalic acid ($H_2C_2O_4 \cdot 2H_2O$) was loaded into a plastic vial (50 mL) with agate milling balls (3–5 mm) under ambient conditions. The weight ratio between the balls and powders was 10:1. The grinding was carried out in a planetary mill (QM-1SP04) at a speed of 600 rpm for 2 h (Scheme 1). After the completion of grinding, the as-ground oxalate precursor was separated from the balls followed by calcination at 300 or 500 °C in air for 4 h. The final calcined samples were designated as GO-T, where T stands for the calcination temperature (see Table 2). Following the same procedure, with the main difference being the ball/powder ratio changed to 20/1 or the use of citric acid in place of oxalic acid, two additional samples labeled as GH-300 (GH strands for grinding with higher milling intensity) and GC-300 (GC stands for grinding using citric acid as the precursor) were prepared, respectively.



$$\tfrac{1}{2}Cu_2(OH)_2CO_3 + MnCO_3 + 2H_2C_2O_4 \cdot 2H_2O \rightarrow CuMn(C_2O_4)_2 + \tfrac{13}{2}H_2O + \tfrac{3}{2}CO_2\uparrow$$

Scheme 1 The soft reactive grinding process based on dry precursor synthesis for the preparation of copper–manganese mixed oxide catalysts

For comparison, two reference $Cu/MnO_x$ catalysts obtained by the wet-chemical methods were prepared. Briefly, the CN-T catalyst was prepared by aqueous hydroxycarbonate coprecipitation according to a method described elsewhere [16]. In short, a 1.2 M aqueous solution of $NaCO_3$ was added into an aqueous solution of Cu and Mn nitrates (each 0.5 M) under vigorous stirring. The temperature was kept at 80 °C during precipitation and maintaining the pH at 8.5. The precipitates were washed thoroughly and dried in air at 110 °C for 12 h, followed by calcination at 300 or 500 °C in air for 4 h. The CO-T catalyst was prepared by oxalate-coprecipitation in aqueous solution according to a method described in Ref. [27]. Briefly, a certain amount of copper nitrate and manganese nitrate were dissolved in water and aqueous solution of 20% excess of oxalic acid was injected rapidly into the solution at room temperature under vigorous stirring. The resultant precipitates were dried at 110 °C overnight, followed by calcination at 300 or 500 °C for 4 h.

### 2.2 Catalyst Characterization

The BET specific surface areas of the calcined samples were determined by adsorption–desorption of nitrogen at liquid nitrogen temperature, using a Micromeritics TriStar 3000 equipment. Sample degassing was carried out at 300 °C prior to acquiring the adsorption isotherm. The powder X-ray diffraction (XRD) measurement was carried out on a Bruker D8 Advance X-ray diffractometer using nickel filtered CuKα radiation (1.5406 Å) with a scanning angle ($2\theta$) of 15–80°, a scanning speed of 0.84° min$^{-1}$, a voltage and current of 40 kV and 20 mA, respectively. TPR measurements were carried out on a homemade apparatus as described elsewhere. About 20 mg of a freshly calcined catalyst was mounted in a quartz tube. TPR experiments were carried out in 5% H$_2$/Ar flowing at 40 mL min$^{-1}$, with a ramping rate of 10 °C min$^{-1}$. Diffuse reflectance infrared Fourier transform spectroscopy (DRIFTS) characterization of the catalysts was performed using a Bruker Vector 22 spectrometer equipped with a DTGS detector and a KBr beam splitter. The samples were placed in a sample cup inside a Harrick diffuse reflectance cell equipped with ZnSe windows and a thermocouple mount that allowed direct measurement of the sample temperature. All spectra were collected in dry air atmosphere at room temperature.

### 2.3 Activity Tests

Steam reforming of methanol was carried out in a fixed-bed micro-reactor at atmospheric pressure and reaction

temperatures in the range of 220–300 °C. All runs were performed using 0.5 g of catalyst diluted with 0.5 g quartz sand (both in 40–60 mesh). After reduction in a $H_2/Ar$ (5/95) flowing of 40 mL min$^{-1}$ at 250 °C for 2 h, premixed water and methanol with a $H_2O/MeOH$ molar ratio of 1.3 at a flow rate of 44.0 mL-NTP min$^{-1}$ were fed into the preheater maintained at about 240 °C by means of a microfeeder. The vaporized feed entered the reactor with a stream of Ar gas, which had a flow rate of 40 mL min$^{-1}$, and then began the steam reforming reaction at the designated reaction temperature. The reaction products were first passed through a cold trap, then the gaseous products such as $H_2$, CO, $CO_2$ were detected on-line by the gas chromatograph (Type GC-122, Shanghai Analysis) equipped with thermal conductivity detector (TCD) and TDX-01 column; the liquid products such as water, methanol were analyzed by the same Gas Chromatograph equipped with another TCD detector and Porapak-Q column. Unless otherwise mentioned, the catalytic activity was evaluated from the data collected after 5 h of the on-stream operation by methanol conversion ($X_{MeOH}$), $CO_2$ selectivity ($S_{CO2}$) and CO selectivity ($S_{CO}$) in the outlet.

## 3 Results and Discussion

### 3.1 Characterization of the Catalysts

XRD measurements of the mechanochemical activation of the starting carbonates of copper/manganese salts with oxalic acid showed that the formation of a complex oxalates starts within the initial minutes of activation (Scheme 1). Figure 1a presents the XRD pattern of the grinding-derived Cu–Mn mixed oxalate precursors

(GO-AS) prepared by a short grinding time of 2 h. For comparison, the XRD results of the single copper oxalate and manganese oxalate prepared in the same way as well as the mixed oxalate precursors (CO-AS) obtained by conventional aqueous oxalate coprecipitation are also given in Fig. 1b–d, respectively. Notice that the XRD results of the CO-AS sample prepared by the wet-chemical method is apparently a simple mixture of the single phases of copper oxalate and manganese oxalate. In sharp contrast to the diffraction patterns as observed for the pure oxalate phases or the CO-AS sample, additional diffraction features (asterisked peak as shown in Fig. 1a) corresponding to a single-phase mixed oxalate have been identified with the GO-AS sample prepared by the soft reactive grinding method. This single-phase mixed oxalate phase is possibly due to a substantial mechanochemically induced isomorphous substitution between copper and manganese oxalate phases and is expected to contribute the formation of well-defined Cu–Mn spinel oxides [26]. Moreover, the absence of characteristic peaks of the starting carbonate precursors in the as-ground powder is an indication of the completion of the solid reaction [26].

Figure 2a compares the XRD patterns of calcined catalyst precursors obtained by the SRG and conventional aqueous coprecipitation methods, illustrating that the phase properties of the copper–manganese oxide catalysts varied significantly depending on the preparation method employed. The X-ray diffraction data of samples GO-300 and GO-500 reveal a predominant $Cu_{1.5}Mn_{1.5}O_4$ spinel phase together with a minor CuO phase of the SRG-derived materials. The spinel $Cu_{1.5}Mn_{1.5}O_4$ phase is a non-stoichiometric form of $CuMn_2O_4$ and it is usually expressed as $Cu_xMn_{3-x}O_4$ or $Cu_{1+x}Mn_{2-x}O_4$ [4]. It is noteworthy that the generation of well-defined Cu–Mn spinel phase could

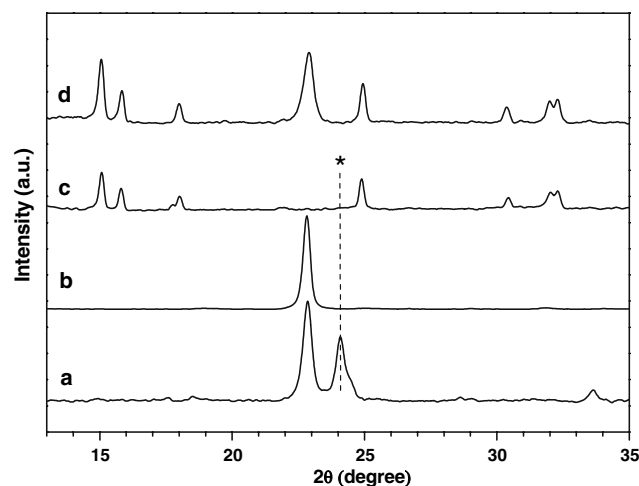**Fig. 1** X-ray diffraction patterns of Cu/Mn mixed oxalate precursors prepared by dry and wet-chemical methods: (a) GO-AS; (b) $CuC_2O_4 \cdot nH_2O$; (c) $MnC_2O_4 \cdot nH_2O$; (d) CO-AS
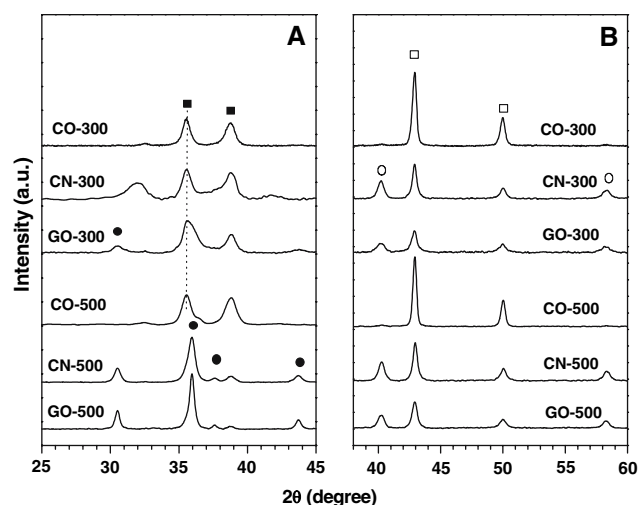
**Fig. 2** XRD profiles of the various $Cu/MnO_x$ catalysts before (**a**) and after (**b**) reaction. (●) $Cu_{1.5}Mn_{1.5}O_4$; (■) CuO; (□) Cu; (○) MnO
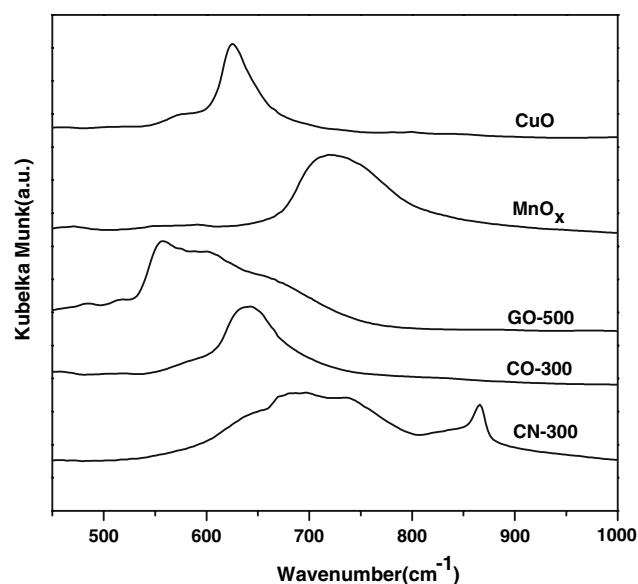
**Fig. 3** DRIFT spectra of the Cu/Mn mixed oxides prepared by dry and wet-chemical methods after calcination at 300 °C

be favourably achieved for the SRG-derived materials at an extremely low calcination temperature of 300 °C, in contrast to the way in which temperatures higher than 500 °C is required for conventional wet-chemically derived CO-$T$ or CN-$T$ samples in obtaining the Cu–Mn spinel phases. At this situation, it should be noted that the diffraction peaks characteristics of crystalline $Mn_2O_3$ or $Mn_3O_4$ oxides cannot be identified in all samples, suggesting a high dispersion or an amorphous nature of the manganese oxide species [28].

To gain a further insight into the structural evolution of the calcined samples prepared by different methods, the DRIFTS measurements were preformed. Figure 3 shows the spectra of Cu–Mn mixed oxide catalysts together with those of CuO and $MnO_x$ pure oxides included as reference. CO-300 presents a broad band at 620 cm$^{-1}$ which coincides well with that of pure CuO. For CN-300, a broader band at 700 cm$^{-1}$ appears by the contribution of the bands at 720 cm$^{-1}$ of Mn–O. A sharp band at 875 cm$^{-1}$ characteristic of the vibrations of $CO_3^{2-}$ confirmed the presence of residual copper and manganese carbonates. One additional band at 550 cm$^{-1}$ in sample GO-300 could be ascribed to a particular vibrational feature of the $Cu_{1.5}Mn_{1.5}O_4$ [13, 28], besides the broad bond of CuO. The observation is consistent with the XRD results as shown in Fig. 2a. Thus, coupled with the XRD data, the observation of the IR band characteristics of $Cu_{1.5}Mn_{1.5}O_4$ spinel phase clearly demonstrate that the SRG technique based on dry oxalate-precursors synthesis can allow a facile and favorable preparation of Cu–Mn spinel materials by a direct precursor-calcination at temperatures substantially lower than conventional methods.

In order to investigate the active phase of the Cu/$MnO_x$ catalysts for SRM reaction, the XRD patterns of the six catalysts after reduction followed by subsequent reaction at 240 °C were collected and shown in Fig. 2b. Evidently, metallic copper phase is observed for all the samples after reaction, with additional MnO phase being identified in GO- and CN-series samples. This indicates that the metallic copper is the active phase of the present Cu/$MnO_x$ catalysts for SRM reaction [29, 30]. Assuming that Cu particles were spherical, the average copper metal crystallite sizes were calculated from the FWHM of Cu (111) diffraction lines. As far as the 300 °C-calcined samples is concerned, the calculation results reveal a much smaller copper particle size for GO-300 (15 nm) as compared to CN-300 (20 nm) and CO-300 (24 nm). The variation of the copper particle size for the 500 °C-calcined samples followed the same trend of the samples obtained by calcination at 300 °C, i.e., GO-500 (17 nm) < CN-500 (24 nm) < CO-500 (30 nm). Moreover, it is noticeable that only a slight copper nanoparticle size increase from 15 to 17 nm was evidenced for GO-300 and GO-500 samples, in sharp contrast to the much larger Cu particle size increase as identified for their conventional counterparts. All these observations, in combination with the accelerated ageing tests for the SRM reaction presented below, strongly suggest that the present grinding-derived Cu–Mn spinel catalysts can afford the favorable creation of much smaller Cu nanocrystals with improved thermal stability in the active catalysts.

Temperature-programmed reduction experiments were carried out to investigate the reducibility of the various Cu–Mn mixed oxide materials. Figure 4 reported the influence of preparation method on the redox properties of the Cu–Mn catalysts. All samples exhibit a broad reduction profile together with shoulders in the temperature range 150–350 °C. The reduction of bulk CuO is featured by a single reduction peak at a considerably higher temperature of 320 °C (not shown). It is thus concluded that there is a Cu/Mn interaction which facilitates the reduction of the supported copper species. In order to gain a further insight into the TPR results, the profiles of the samples containing $Cu_{1.5}Mn_{1.5}O_4$ spinel phase are deconvoluted using a computer program [31]. The peak positions and their contributions derived from deconvolution are summarized in Table 1. The original TPR profile can be deconvoluted into at least three peaks in all cases. This suggests the presence of at least two types of copper or manganese phase in the Cu/$MnO_x$ samples, where dispersed or crystallized CuO phase ($\alpha$ peak), $Cu_{1.5}Mn_{1.5}O_4$ spinel phase or $MnO_x$ strongly interacted with the spinel phase ($\beta$ and $\gamma$ peaks) co-exist. The fraction of medium temperature reduction peak, i.e., the $\beta$ peak, is observed to be the highest and shifted to significantly lower temperatures for
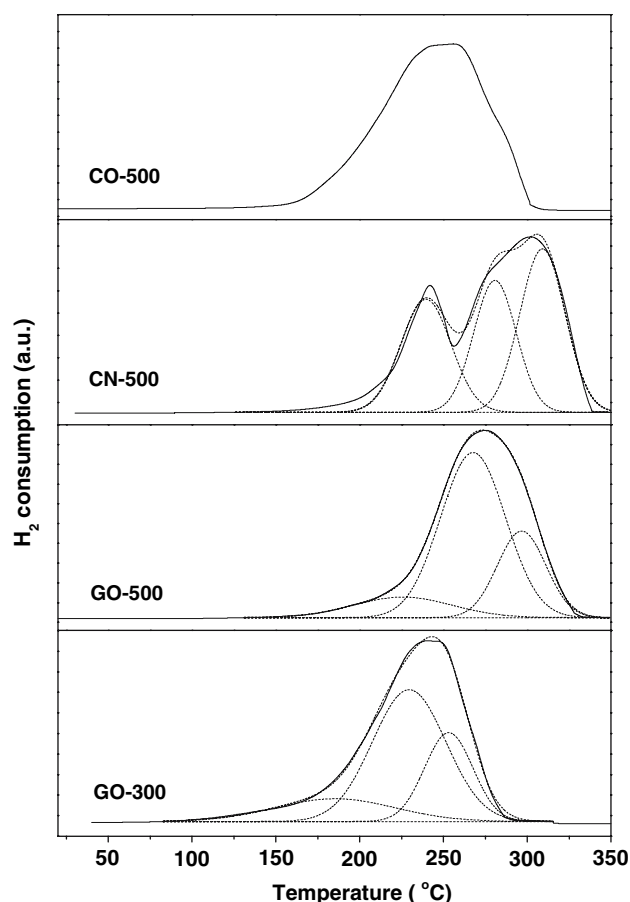
**Fig. 4** TPR profiles of the $Cu/MnO_x$ catalysts prepared by different methods

sample GO-300 as compared to the conventional coprecipitation-derived spinel samples, indicating the presence of a stronger Cu/Mn interaction in the sample prepared by SRG method.

Table 2 shows the surface area for each catalyst examined in this work. It is shown that the BET surface area prepared by grinding route is much larger than those of the catalysts obtained by coprecipitation calcined at the same temperature. Comparison of the grinding-derived samples using different grinding parameters reveals that catalyst GH-300 has a much larger specific surface area than its grinding-derived counterparts prepared under much milder milling conditions. Note that the specific surface area ($S_{BET}$) and pore volume of the GH-300 sample containing well-defined $Cu_{1.5}Mn_{1.5}O_4$ spinel phase was found to be ca. 118 $m^2 g^{-1}$, much higher than the reported one obtained by conventional wet-chemical or combustion methods [28, 29]. The effect of the calcination temperature on specific surface area for the present Cu–Mn mixed oxide sample is dramatic as reported for conventional aqueous coprecipitation-derived materials in the literature [3, 16, 32]. It is seen that the $S_{BET}$ of catalyst GO-500 is

drastically reduced to 25 $m^2 g^{-1}$, being significantly lower than that of the GO-300 sample. Nevertheless, this value is still much higher than its 500 °C calcined-analogues obtained by aqueous coprecipitation route. Thus, it can be concluded that thermally stable Cu–Mn spinel catalysts with favorable textural properties could be obtained in the present study.

## 3.2 Catalytic Activity

The catalytic activity, selectivity and stability of the resultant nanostructured Cu–Mn spinel oxides are tested for the steam reforming of methanol, which represents a promising alternative for use in catalytic generation of high purity hydrogen to produce clean electrical energy from fuel cells for vehicles applications [33]. The conventional Cu/ZnO-based catalysts often have disadvantages, such as low thermal stability and the requirement of temperatures as high as 280 °C for efficient operation [34]. From a practical viewpoint, it is desirable to operate the reformer at lower reaction temperatures due to the temperature mismatch between the reactor and the fuel cell. Moreover, the high reaction temperature tends to result in the production of CO—a poison to the promising proton-exchange membrane (PEM) fuel cells [35, 36]. Thus, new improved catalyst systems that can allow the effective production of hydrogen free from carbon monoxide at lower reaction temperatures are highly desired. Table 2 shows that the catalytic activity of the SRG-derived Cu–Mn mixed oxide materials for the SRM reaction strongly depends on the milling intensity and complex precursors during reactive grinding synthesis. Interestingly, the Cu–Mn spinel catalyst prepared via oxalate precursors is found to be extremely active, successfully converting more than 92% of methanol at temperatures around 240–260 °C. As a comparison, in the same reaction temperature range, the spinel materials prepared via citrate precursors can only convert 68% of $CH_3OH$. Moreover, it is obvious that the samples prepared by 300 °C calcination always have higher SRM activity than the 500 °C-calcined ones. The superior activity of GO-300 catalyst prepared via soft reactive grinding is

**Table 1** TPR peak positions and concentrations of reducible species in the Cu–Mn mixed oxide catalysts as determined by the deconvolution of TPR profiles

| Catalyst | TPR peak position (temperature °C) and fraction (%) | | |
| --- | --- | --- | --- |
| | Peak $\alpha$ | Peak $\beta$ | Peak $\gamma$ |
| GO-300 | 185 (16.3) | 230 (58.0) | 253 (25.7) |
| GO-500 | 226 (11.9) | 268 (63.4) | 297 (24.7) |
| CN-500 | 240 (30.3) | 281 (30.1) | 309 (39.7) |

**Table 2** Physicochemical properties and catalytic performance of various Cu–Mn mixed oxide catalysts for methanol steam reforming[a]

| Catalytic system | $S_{BET}$ ($m^2 g^{-1}$) | $V_{pore}$ ($cm^3 g^{-1}$) | $d_{pore}$ (nm) | Reaction temperature (°C) | MeOH conversion (%) | CO selectivity (%) | $H_2$ selectivity (%) | $H_2$ production rate (mmol $g_{cat}^{-1}$ $h^{-1}$) |
|---|---|---|---|---|---|---|---|---|
| GO-300 | 96.1 | 0.35 | 12.5 | 240 | 74.0 | 0.8 | 99.4 | 226 |
|  |  |  |  | 260 | 88.5 | 0.8 | 99.4 | 270 |
| GO-500 | 24.6 | 0.18 | 26.5 | 240 | 65.2 | 1.3 | 99.1 | 199 |
|  |  |  |  | 260 | 80.5 | 1.5 | 99.4 | 246 |
| CN-300 | 55.2 | 0.14 | 8.5 | 240 | 51.5 | 1.2 | 99.6 | 157 |
|  |  |  |  | 260 | 65.7 | 1.1 | 99.1 | 201 |
| CN-500 | 14.9 | 0.07 | 18.5 | 240 | 45.5 | 1.7 | 99.4 | 139 |
|  |  |  |  | 260 | 61.8 | 1.5 | 99.1 | 189 |
| CO-300 | 9.6 | 0.06 | 18.2 | 240 | 42.9 | 1.5 | 99.1 | 131 |
|  |  |  |  | 260 | 59.7 | 1.4 | 99.1 | 182 |
| CO-500 | 4.7 | 0.05 | 34.6 | 240 | 34.7 | 1.5 | 99.1 | 106 |
|  |  |  |  | 260 | 52.5 | 1.5 | 99.4 | 160 |
| GH-300 | 118.1 | 0.39 | 11.1 | 240 | 79.9 | 0.7 | 99.5 | 244 |
|  |  |  |  | 260 | 92.9 | 0.7 | 99.5 | 284 |
| GC-300 | 60.6 | 0.30 | 17.5 | 240 | 56.7 | 1.5 | 99.4 | 173 |
|  |  |  |  | 260 | 68.6 | 1.6 | 99.6 | 209 |

[a] Reaction conditions—$CH_3OH$: 19 mL-NTPmin$^{-1}$, $H_2O$: 25 mL-NTPmin$^{-1}$, Ar: 20 mL-NTPmin$^{-1}$, $H_2O/CH_3OH$ = 1.3/1, P = 0.1 MPa

believed to be attributed to the beneficial generation of catalytically active $Cu_{1.5}Mn_{1.5}O_4$ spinel phase as well as the high surface area nature of the material, which provides higher component dispersion as well as much smaller Cu nanocrystals due to a stronger metal-support interaction in the working catalyst. The catalytic performance of the Cu–Mn mixed oxides obtained by conventional aqueous coprecipitation are much inferior to the SRG-derived samples, possibly because of the lower surface areas and the presence of less of the active phase of $Cu_{1.5}Mn_{1.5}O_4$ spinel. Furthermore, as shown in Fig. 5, the SRG-derived Cu–Mn spinel oxides also demonstrate very high thermal stability by maintaining its extremely high activity even after thermally aged at 350 °C for 40 h. As a comparison, a SRG-derived Cu/ZnO catalyst obtained by a 8 h reactive grinding synthesis (see Ref. [26]) is substantially deactivated when it is subjected to the same treatment, although its initial activity achieves more than 78.8% methanol conversion. Hence, these newly synthesized nanostructured Cu–Mn spinel oxides are proven to be superior in catalytic activity, $H_2$ selectivity, and stability for the steam reforming of methanol, as compared to the widely studied Cu/ZnO-based catalysts with poor thermal stabilities. Thus, the SRG-derived Cu–Mn spinel oxides demonstrate great potential for practical applications in catalytic generation of high purity hydrogen used in fuel cells for vehicles applications.
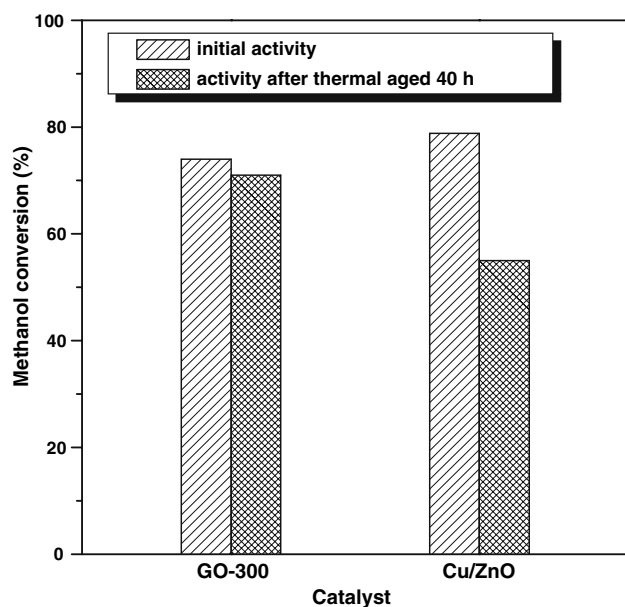


**Fig. 5** Influence of accelerated ageing on the methanol conversion rates of catalysts for the steam reforming of methanol. Conditions—$CH_3OH$: 19 mL-NTPmin$^{-1}$, $H_2O$: 25 mL-NTPmin$^{-1}$, Ar: 20 mL-NTPmin$^{-1}$, $H_2O/CH_3OH$ = 1.3/1, P = 0.1 MPa

## 4 Conclusions

In summary, we successfully demonstrate the synthesis of Cu–Mn spinel oxide catalysts by a waste-free soft reactive grinding method, based on the facile dry activation of

non-toxic and inexpensive inorganic precursor salts. The superior performance of the dry-synthesized Cu–Mn spinel catalysts in the methanol steam reforming for hydrogen production, as compared with the conventional material obtained by aqueous coprecipitation, has been attributed to the generation of catalytically active $Cu_{1.5}Mn_{1.5}O_4$ spinel phase with a high surface area in the grinding-derived samples. The most apparent advantage of the present solvent-free SRG technology is that it does not need high-energy consumption, long preparative time, tedious multi-step processing or conventional toxic-release precursor salts as the starting materials, thus providing new environmentally friendly and cost-reductive approach for preparing industrially important Cu–Mn spinel catalyst systems.

## References

 1. Mirzaei AA, Shaterian HR, Habibi M, Hutchings GJ, Taylor SH (2003) Appl Catal A 253:499
 2. Krämer M, Schmidt T, Stöwe K, Maier WF (2006) Appl Catal A 302:257
 3. Tanaka Y, Utaka T, Kikuchi R, Takeguchi T, Sasaki K, Eguchi K (2003) J Catal 215:271
 4. Morales MR, Barbero BP, Cadús LE (2006) Appl Catal B 67:229
 5. Kang M, Park ED, Kim JM, Yie JE (2006) Catal Today 111:236
 6. Wang F, Yang G, Zhang W, Wu W, Xu J (2003) Chem Commun 1172
 7. Wang F, Yang G, Zhang W, Wu W, Xu J (2004) Adv Synth Catal 346:633
 8. Han YF, Ramesh K, Chen LW, Widjaja E, Chilukoti S, Chen FX (2007) J Phys Chem C 111:2830
 9. Ramesh K, Chen LW, Chen FX, Zhong ZY, Chin JH, Mook HW, Han YF (2007) Catal Comm 8:1421
10. Han YF, Chen FX, Zhong ZY, Ramesh K, Chen LW, Chin JH, Widjaja E (2006) Catal Comm J Phys Chem B 110:24450
11. Papavasiliou J, Avgouropoulos G, Ioannides T (2007) J Catal 251:7
12. Papavasiliou J, Avgouropoulos G, Ioannides T (2005) Catal Commun 6:497
13. Spassova I, Khristova M, Panayotov D, Mehandjiev D (1999) J Catal 185:43
14. Schwab G, Kanungo S (1977) J Phys Chem 107:109
15. Li XQ, Xu J, Zhou LP, Wang F, Gao J, Chen C, Ning JB, Ma H (2006) Catal Lett 110:149
16. Hutchings GJ, Mirzaei AA, Joyner RW, Siddiqui MRH, Taylor SH (1998) Appl Catal A 166:143
17. Schwarz JA (1995) Chem Rev 95:477
18. Hagen A, Schneider E, Kleinert A, Roessner F (2004) J Catal 222:227
19. Salou M, Kooli F, Kiyozumi Y, Mikamizu F (2001) J Mater Chem 11:1476
20. Salou M, Kiyozumi Y, Mikamizu F, Nair P, Maeda K, Niwa S (1998) J Mater Chem 8:2125
21. Huang L, Kramer GJ, Wieldraaijer W, Brands DS, Poels EK, Castricum HL, Bakker H (1997) Catal Lett 48:55
22. Kaliaguine S, Neste AV, Szabo V, Gallot JE, Bassir M, Muzychuk R (2001) Appl Catal A 209:345
23. Bulushev DA, Minsker LK, Zaikovskii VI, Renken A (2000) J Catal 193:145
24. Boldyrev VV, Tkacova K (2000) J Mater Synth Process 8:121
25. Trovarelli A, Zamar F, Llorca J, Leitenburg C, Dolcetti G, Kiss JT (1997) J Catal 169:490
26. Wang LC, Liu YM, Chen M, Cao Y, He HY, Wu GS, Dai WL, Fan KN (2007) J Catal 246:193
27. Zhang XR, Wang LC, Cao CZ, Cao Y, Dai WL, He HY, Fan KN (2005) Catal Lett 102:183
28. Puckhaber LS, Cheung H, Cocke DL, Clearfield A (1989) Solid State Ionics 32/33:206
29. Ning WS, Shen HY, Liu HZ (2001) Appl Catal A 211:153
30. Tabatabaei J, Sakakini BH, Watson MJ, Waugh KC (1999) Catal Lett 59:143
31. Yao CZ, Wang LC, Liu YM, Wu GS, Cao Y, Dai WL, He HY, Fan KN (2006) Appl Catal A 297:151
32. Ishikawa T, Ohashi R, Nakabayashi H, Kakuta N, Ueno A, Furuta A (1992) J Catal 134:87
33. Papavasilious J, Avgouropoulos G, Ioannides T (2006) Appl Catal B 66:168
34. Mascaros SM, Navarro RM, Sainero LG, Costantino U, Nocchetti M, Fierro JLG (2001) J Catal 198:338
35. Agrell J, Boutonnet M, Fierro JLG (2003) Appl Catal A 253:213
36. Suzuki VK, Okazaki M, Kapoor MP, Osaki T, Ohashi F (2000) J Catal 194:373